

Design and Analysis of a Waveguide Structure for 211-275 GHz 2SB SIS Mixer

Andrey Khudchenko, Ivan Tretyakov, Valery P. Koshelets, Ronald Hesper and Andrey M. Baryshev

Abstract—We present an analysis of a waveguide structure for a 211-275 GHz Sideband Separating (2SB) mixer based on SIS tunnel junctions. A general analytical model describing a quality of Sideband Rejection Ratio (SRR) is developed. It shows a crucial influence of reflections from single-ended mixers, RF load and the RF hybrid on the SRR level. Due to intrinsic asymmetry of 2SB waveguide structure, the reflections strongly affect both the balance of the observed signal and the balance on the LO pumping signal. The model is verified and confirmed by 3D electromagnetic simulations showing good qualitative and quantitative agreement. The developed theory gives a practical tool to design 2SB waveguide mixers with a required SRR level. Based on the presented theory, the waveguide structure of the 211-275 GHz 2SB SIS mixer is designed. It is predicted a degradation of SRR level from 26 dB to about 18 dB due to reflections. The developed model explains some experimental data measured for 2SB SIS mixers developed earlier.

Index Terms—Sideband separating (2SB) mixers, sideband rejection ratio (SRR), submillimeter wave technology, terahertz receivers, superconductor-insulator-superconductor junctions.

I. INTRODUCTION

SIDEBAND separating (2SB) receivers based on superconductor-insulator-superconductor (SIS) mixers are widely used in ground-based astronomy: ALMA [1], NOEMA and APEX [2], just to name a few. A Sideband Rejection Ratio (SRR) as high as 20 dB is desirable for improved receiver sensitivity. However, the typical SRR specification is only 10 dB [3] due to technical issues, and in fact many groups developing receivers for ALMA have struggled to meet this specification. The focus has been on optimizing balance of the individual receiver components: RF and IF hybrids and mixers gain. The imbalance of each part has been reduced to a level below 0.5 dB. Still, a total imbalance of 1.5 dB would give the SRR better than 20 dB across the band, but in reality it was only 10 dB at the worst points [4], [5]. In this work we have focused in studying the SRR

Manuscript received [—]; revised [—]; accepted [—]. Date of publication [—]; date of current version [—]. This work was supported by a grant from the Russian Science Foundation (project No. 23-79-00061, <https://rscf.ru/project/23-79-00061/>). The equipment of USU number 352529 “Cryointegral” was used to perform the simulations, USU was supported by the Ministry of Science and Higher Education of Russian Federation under Grant 075-15-2021-667.

A. Khudchenko, I. Tretyakov, are with the Astro Space Center of P.N. Lebedev Physical Institute of Russian Academy of Science, 119991, Moscow, Russia (e-mail: Khudchenko@asc.rssi.ru; tretyakov@asc.rssi.ru).

V.P. Koshelets, is with the Kotel'nikov Institute of Radioengineering and Electronics RAS, 125009, Moscow, Russia (e-mail:valery@hitech.cplire.ru)

A.M. Baryshev, R. Hesper are with the Kapteyn Astronomical Institute, University of Groningen, Groningen, 9747 AD, The Netherlands (e-mail: A.M.Baryshev@astro.rug.nl).

Digital Object Identifier [—]

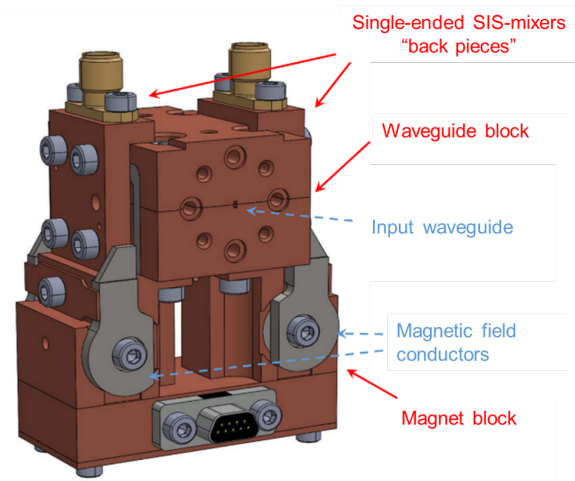


Fig. 1. Model of the modular 2SB mixer block combining RF waveguide block, two back pieces equipped with the SIS devices and two magnet blocks for suppression of the critical current in the SIS junctions.

pattern of the 2SB receiver to determine the cause of its degradation. In addition we apply the developed methods to design the waveguide structure of a 211-275 GHz 2SB mixer based on SIS devices.

The development of the 2SB mixer started some time ago as a Russian-Dutch joint initiative to facilitate LLAMA telescope [6] with a high quality receiver. This instrument could be used also in the Millimetron space mission [7]. A DSB SIS mixer with a good performance has been demonstrated recently [8], [9]. In this paper we perform the design of a waveguide part for the 2SB receiver has been performed as the next step of the receiver development.

II. WAVEGUIDE BLOCK DESIGN

For the 211-275 GHz 2SB mixer we chose a modular design approach, a similar to the one used for the 600–720 GHz 2SB mixer [10], [11], or to the one used recently for 300–360 GHz mixer [12]. In this design concept, the critical components such as the RF hybrid block, RF horn, LO horn and SIS junctions mounted in holders (“back pieces”), are designed as independent units. This enables convenient characterization of the individual parts leading to better matching. The designed RF block is shown in Fig.1.

The waveguide structure is based on a standard quadrature hybrid architecture, which is integrated with two LO couplers and an LO splitter into a classical E-plane waveguide split-block [11], as shown in Fig 2. We chose a 1000x500 μm

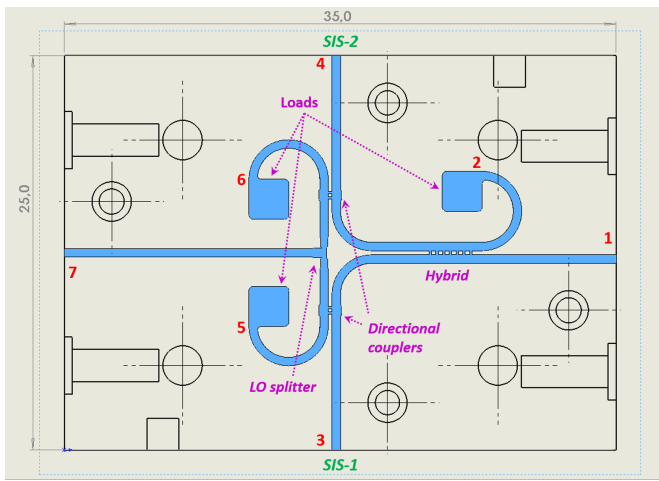


Fig. 2. Drawing of the hybrid block showing the RF waveguide structure. Ports 1 and 7 show the inputs for the LO and RF signals correspondingly. Ports 3 and 4 are associated with signs “SIS-1” and “SIS-2”, which indicate the location of the SIS junctions after the back pieces are installed. Ports 2, 6, 5 show the loads: 2 - RF load to suppress parasitic reflections, 6 and 5 - LO loads dump the unused LO power. The waveguide block size is 25 x 35 mm.

TABLE I
DIMENSIONS OF KEY WAVEGUIDE STRUCTURES SHOWN IN FIG.3

Hybrid		LO coupler		LO split	
Dimension	μm	Dimension	μm	Dimension	μm
b	500	b	500	b	500
s	290	s	276	ri	80
$p1$	428	$p1$	183	$w0$	587
$p2$	856	$g0$	108	$w1$	259
$p3$	1284	sw	560	$w2$	394
$g0$	124	sh	67	$E0$	649
$g1$	124	ri	80	$E1$	415
$g2$	116			$E2$	1039
$g3$	108				

waveguide to cover the 211–275 GHz frequency band. These dimensions locate the operational band in the high-frequency end of the one-octave single-mode waveguide range in order to minimize waveguide losses. Furthermore, this feature has insured compatibility with our previously developed mixer back pieces [8], [9].

To build a high-quality 2SB receiver one should pay particular attention to the phase and amplitude balance of the entire RF structure, since RF imbalance is the key parameter that limits the Sideband Rejection Ratio (SRR). Based on our previous research on 2SB SIS mixers [10], [13], [14], we have discovered that the total RF balance is strongly affected by reflections within the RF structure, rather than by the pure amplitude and phase balance of the RF hybrid itself. This effect will be clearly proven below in this article. As a result, besides hybrid balance, we have focused on maximizing of hybrid isolation. The performances of all the waveguide components have been calculated using the electromagnetic 3D simulator HFSS.

1) *Quadrature Hybrid*: The quadrature hybrid (Fig. 3, top) is a seven-branch coupler. As stated previously, one of the main objectives of the design goals was the reducing of the isolation (here labelled S_{21} ; the port numbers are indicated

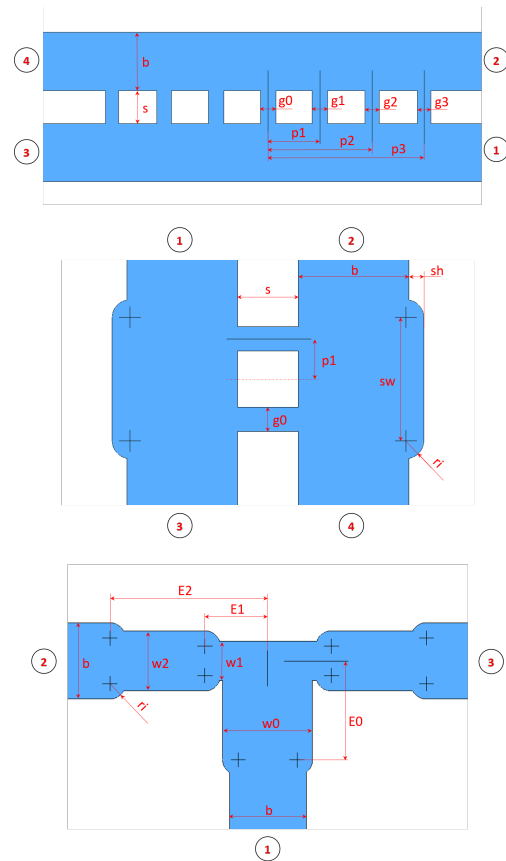


Fig. 3. Layout of the quadrature hybrid (top picture), LO coupler (middle picture) and the LO splitter (bottom picture). The dimensions are shown in Table I. The numbers in circles denote the port numbers as referred in the text.

in the figure). To achieve this, the dimensions were optimised (mainly slot widths and positions), while ensuring that the phase and amplitude balance remained within acceptable limits (approximately 0.5° and 1 dB, respectively). While optimizing, it was discovered that the level of (S_{11}) and (S_{21}) strongly depends on the phase balance in a well balanced hybrid. Hence, minimizing the phase error one gets guaranteed lower reflection and isolation of the hybrid.

A representative set of simulated S -parameters is shown in Fig. 4 (top plot). The gain and phase balance are presented in the bottom plot. The gain balance is calculated as $|S_{31}|^2/|S_{41}|^2$; and the phase balance as $\arg(S_{31})-\arg(S_{41})$. The isolation $|S_{21}|^2$ was optimized to be below -26 dB within the band. At the same time, the gain and phase errors are within ± 1 dB and $\pm 0.3^\circ$, respectively. The RF hybrid's contribution to the SRR is derived from the S -parameters using formula:

$$SRR = 20 \cdot \log_{10} \frac{|S_{41} + iS_{31}|}{|S_{41} - iS_{31}|}, \quad (1)$$

which provides the sideband rejection ratio when all the other components of entire 2SB mixer (including IF hybrid, etc.) are perfect. The sideband ratio dependence is shown in Fig. 4 (top plot) by the black curve labeled “SRR”. The worst-case point in the band is approximately -26 dB, which sets the

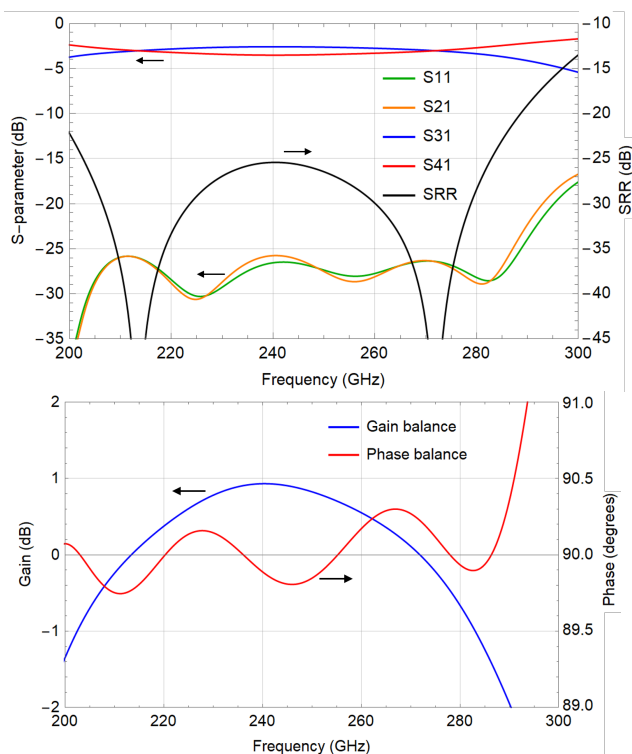


Fig. 4. S-parameters of the simulated hybrid and the hybrid's contribution to the image rejection ratio (top plot). Because of symmetry, each of the other S-parameters is identical to one of the four plotted ones. The bottom plot shows the gain balance and the phase balance.

upper limit for the overall image rejection attainable with this design.

2) *LO Couplers*: The LO is coupled with a classical two-branch directional coupler, shown schematically in Fig. 3, middle panel. The design is similar to the LO coupler for the 650 GHz band described in [13]. It is scaled and slightly modified to provide a wider bandwidth. The coupling factor is set at a level of -16 dB to reduce the insertion loss to about 0.1 dB. With the power provided by commercial sources (several milliwatts in this range), this is more than sufficient to pump the SIS mixers optimally.

3) *LO splitter*: The LO signal is divided equally between the SIS junctions using an E-plane T-splitter, where all three branches have matching sections, as displayed in the bottom panel of Fig.3. The T-splitter is a non-dissipative three-port device. Consequently, it has both a high reflection in its output ports (S22, S33) and low isolation between them (S23, S32). As both aspects affect the LO standing waves equally, they are set to be about equal (≈ -6 dB). The input reflection of the LO input port (S11) was designed to be below -18 dB for the LO tuning band.

4) *SIS mixers*: For this prototype 2SB mixer we intend to use SIS mixer devices based on standard Nb/AlO/Nb tunnel junctions encapsulated in 250 nm thick Nb microstrip line. The dielectric between the microstrip layers is a 250 nm SiO₂ film. Further information on the SIS mixer design, manufacturing, and characteristics can be found in [8], [9].

5) *RF load*: On the drawing in Fig.2 we have provided cavities for the loads (ports 2, 5, 6). Currently, we are

designing and testing of our cryogenic loads which will be presented later. Still, the importance of the loads, especially the RF load, can not be underestimated as it will be shown below by demonstration of the SRR performance influenced by reflections.

6) *Tolerance analysis*: The waveguide block will be manufactured by micro-milling. For this method, one can expect 2-3 μ m accuracy for the parameters given in Table I. The tolerance analysis for a deviation of 2.5 μ m shows that the most critical part is the Hybrid and the gain balance may worsen by an additional 0.3 dB at maximum. This value will be used in section IV to estimate the degradation of the final SRR level because of an additional gain imbalance between two mixers. For the SRR curve displayed in Fig.4 this would lead to degradation from -26 dB to -23 dB in a worst-case scenario.

III. MODELING OF ENTIRE WAVEGUIDE STRUCTURE

In this section we analyse the entire waveguide structure using 3D electromagnetic simulator, and in the end we verify an analytical model describing key factors determining the SRR pattern of the RF part of the 2SB mixer.

A. Reflections

Some time ago, it was suggested that there is a significant impact of RF reflections on the SRR performance for 2SB SIS mixer for 600-720 GHz band [10]. This was concluded based on an analysis of a set of experimental data. The SRR level there was strongly depending on the losses in the waveguide and the SRR vs frequency curve was clearly periodic in some cases. The renewed design of the hybrid structure with reduced level of the suspected reflections showed a clear improvement of the SRR performance. The sideband rejection level exceeded 15 dB in the entire RF band [13], [14].

The mixers and waveguide components may cause numerous standing waves reflections. However, most of them are symmetrical in terms of the two signal path branches and thus do not affect the amplitude and phase balance. Therefore, they have no impact on the SRR.

Two main ways of creating unbalanced interference were suggested in [10] and [14], as shown in 5 for illustration. "The first way" is when the reflections from every SIS device pass back through the hybrid to interfere constructively at RF load (Fig.2 port 2) and destructively at RF input (port 1). The reflection from the load goes back to the SIS mixers, i.e. to the ports 3 and 4. Careful counting of the 90° phase shifts in the hybrid reveals that, whenever due to the overall phase rotation in the system, the reflected signals always arrive in relative antiphase. Because this mechanism causes opposite error vectors in the two mixers, they have a maximum detrimental effect on the SRR, which is determined by the magnitude of the vector difference between the error signals. "The second way" is from either SIS device to the other through the hybrid's isolation (corresponding to S43 and S34 parameters). Although the phase shifts counting is different, the total effect is precisely the same. The rotation rate of this error signal is different from the first one due to the shorter path length. The periods

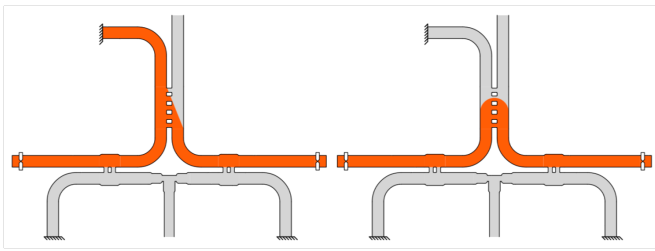


Fig. 5. Schematic illustration of the the two reflection paths in the RF waveguide structure: "the first way" (left side) involves reflection from the RF load, "the second way" (right side) corresponds to "U-turn" in the hybrid. The picture is taken from [14].

TABLE II
REFLECTION FORM THE INTERFACE WITH A WAVEGUIDE OF REDUCED HEIGHT

No	waveguide height (μm)	$ S_{11} ^2$ (dB)
1	100	-3.35.. -3.45
2	190	-6.58.. -6.80
3	250	-9.09.. -9.36
4	410	-19.80.. -19.97

of these two mechanisms are determined by the total length of the corresponding waveguide paths. They were shows to be in a good agreement with the experimentally determined waves in pumping balance of the mixers [10]. Interestingly, because of the above-mentioned vector nature of the interference, neither of the two mechanisms would result in a periodicity of the SRR, just in an overall deterioration. Surprisingly, the presence of both of them, with different periods, is the reason that an interference pattern appears in the SRR vs frequency pattern.

To simulate the influence of both error signals we imitated the reflection in SIS devices and in RF load by reducing the height of ports 2, 3 and 4. A change in a waveguide height produces a wide-band reflection of a fairly flat level. Table II displays a series of reduced heights with corresponding reflection levels when connected to the waveguide of $500 \mu\text{m}$ height. We used the first three levels to simulate the reflection of SIS-device ranging from 3.4dB to 9.2dB, which is a realistic value. For the RF load the set number 4 was used to simulate the reflection of about -20dB.

B. RF balance

The simulated RF balance of the entire RF waveguide structure with reflection is shown in Fig.6. The balance is drastically degraded, especially in phase. The periodic pattern is very fast and it is simply impossible to avoid bad areas having IF range even only 4 GHz wide. The irregular pattern of both phase and amplitude balance point to a multiple contributions with different periods. The significant increase of the SRR level is clearly shown by the bottom plot in Fig.6.

C. LO balance

In addition, it was found that reflections influence the distribution of LO power between SIS devices. It is expected that standing waves in LO routes should be similar due to mirror symmetry, causing no amplitude or phase difference in

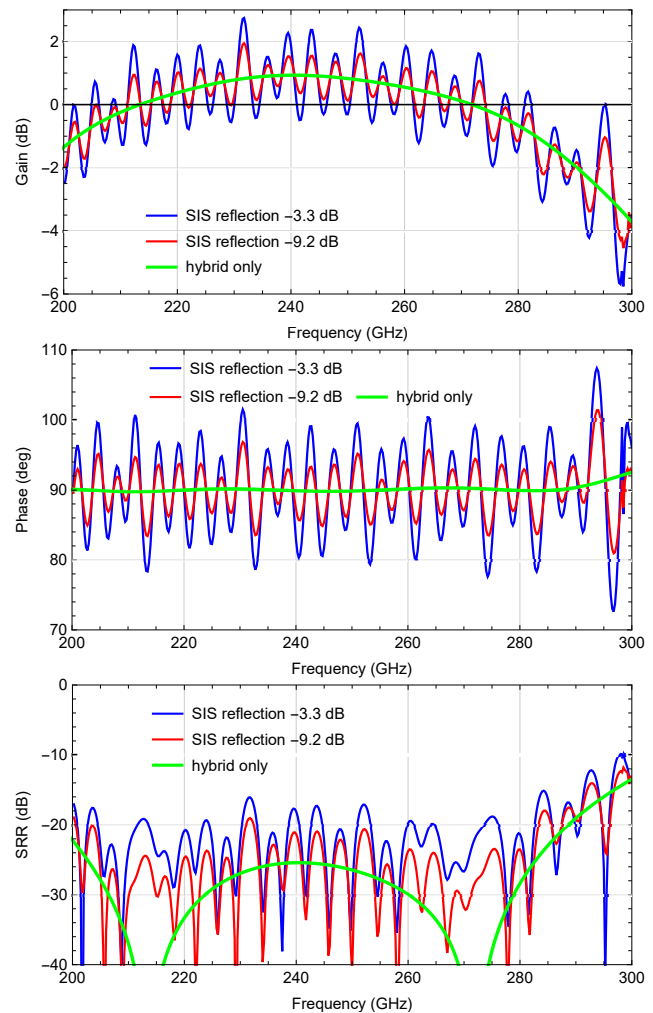


Fig. 6. Simulated amplitude (top plot) and phase (middle plot) balance between the SIS mixers for the entire waveguide structure. The bottom plot shows the SRR dependence on frequency. Blue and red curves are related to the case of SIS reflection of -3.3 dB and -9.2 dB respectively, while RF load reflection stays about -20 dB. Green curves correspond to the single hybrid parameters as presented in Fig.4.

the arriving LO signals at the mixers. However, an analysis of the runs for LO-signal reflections from SIS devices shows that a hybrid's phase flip induces asymmetry, which works similarly to "the first way" interference for the RF signal above. The difference is that LO reflection amplitude will be reduced by a factor of 0.7 because only half of the reflected power will go to the RF load, and the other half is directed to the input horn (port 1 in Fig.2).

It is important to note than, in the case of LO signal the "the second way" interference will not affect the balance, because both the original LO distribution and this type of reflection are mirror-symmetrical and the impact will be the same for both SIS devices.

Simulations of the entire waveguide structure with reflections clearly confirm the suggested LO imbalance. The calculated amplitude and phase balances are demonstrated in Fig.7. The oscillations are similar to the ones in Fig.6 indicating the same nature. The error amplitude in both phase and amplitude is roughly half of that of the RF signal, which

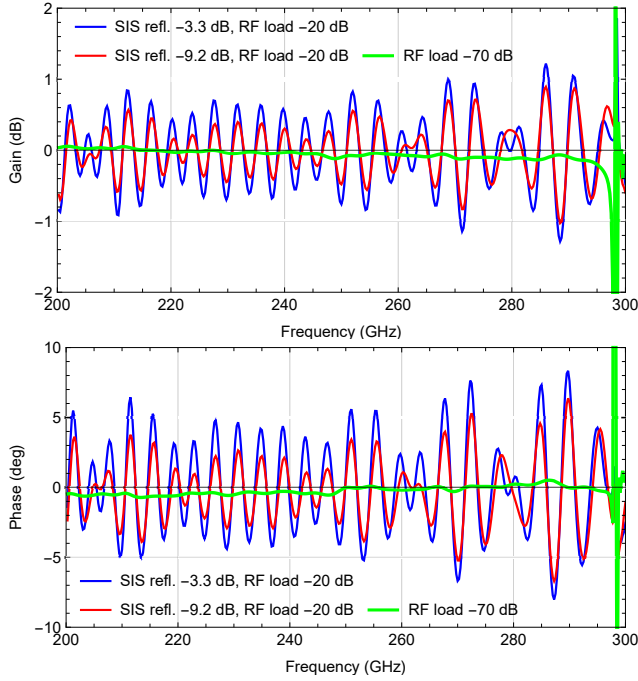


Fig. 7. Simulated amplitude (top plot) and phase (bottom plot) balance of the LO signal between the SIS mixers. Blue and red curves are related to the case of SIS reflection of -3.3 dB and -9.2 dB respectively, while RF load reflection stays about -20 dB. Green curves correspond to the SIS reflection of -3.3 dB and RF load reflection of -70 dB.

is in good agreement with suggestions of 0.7 times lower amplitude for "the first way" interference and absence of "the second way" one. The immunity of the balance to "the second way" interference is also confirmed directly by simulations, see green curves in Fig.7. Here the RF load reflection is -70dB, when SIS reflection stays about -3.3 dB. In this case "the first way" error signal becomes negligibly small, while "the second way" one preserves the same. The simulated level of the gain imbalance is below 0.1 dB and phase error does not go above 0.6 degree. The artifacts around 300 GHz belong to the second harmonic appearing in the directional coupler due to widening of the waveguide. Regardless, it remains outside of the aimed band of 211-275 GHz.

To make a qualitative comparison of the simulated balance with the experimental data published earlier, the plots from [10] are shown in Fig.8. The "RF balance" here corresponds to the inverted gain balance from the top plot in Fig.6, similarly the "LO balance" is associated with the top plot in Fig.7. The qualitative similarity and the presence of the standing waves can be seen. Also, the periodic structure in the "LO balance" measurement could not be explained before, but now the origin and the mechanism of it is clear. The analysis of the measured data is additionally complicated by a manufacturing errors in the waveguide structure.

D. Analytical model

There is a strong motivation to develop an analytical model that describes the balance of the entire RF part of the 2SB mixer. Firstly, while there are a few experimental and simulated facts pointing to the impact of the two proposed error

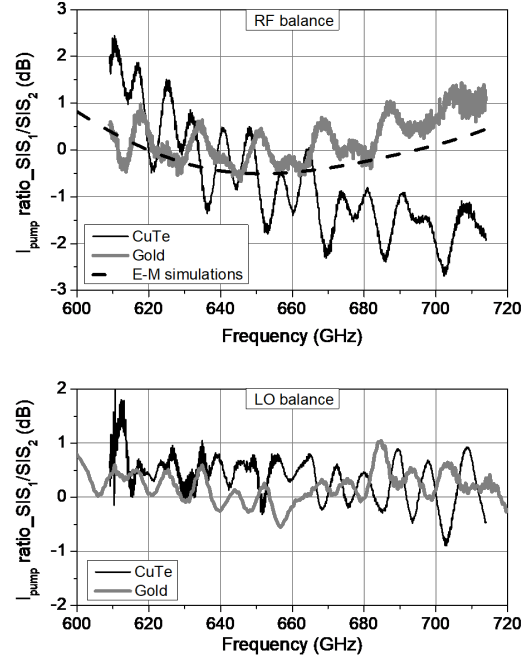


Fig. 8. Figure from [10] showing experimental data for 2SB SIS mixer for ALMA Band 9. Top graph represents the RF gain error, while the bottom one the LO coupling balance: black solid curves are measured for CuTe waveguide block, gray solid curves – for gold-plated one, dashed curve at the top plot shows the result of E-M simulations of the RF hybrid balance. Due to a fabrication error in the hybrid depth, the curve for CuTe RF block on the top plot has a deviation from the E-M simulations.

signals (see section III-A), there has not been confirmation performed yet that is exact and confident. Furthermore, there is no solid proof whether the suggested signals are the only ones giving a significant contribution to the total imbalance. Secondly, the analytical model will provide a much more powerful tool to optimize separate components for the best total performance when compared to simulations of the entire waveguide structure.

The signal arriving directly to the SIS device 1 (see flow chart in Fig.9 and also port 3 in Fig.2) can be written as:

$$S_{31_1} = S_{31_h} \cdot S_c \cdot S_{21_{SIS1}}, \quad (2)$$

here, and further in this section, every S-parameter is a complex function of frequency, S_{31_h} is the S_{31} parameter of the hybrid corresponding to the straight path through ($S_{31} = S_{13} = S_{42} = S_{24}$), S_c is the S_{31} of the directional coupler (similarly, $S_{31} = S_{13} = S_{42} = S_{24}$), and $S_{21_{SIS1}}$ is the coupling coefficient to a SIS mixer 1, which can be estimated for simplicity as $\sqrt{1 - |S_{11_{SIS1}}|^2}$, $S_{11_{SIS1}}$ is the reflection from SIS mixer 1.

"The first way" interference signal arriving to the SIS device 1 consists of two signals S_{31_2} and S_{31_3} (blue and green dashed path in the flow chart in Fig.9), products of reflections from SIS-1 and from SIS-2 respectively, and later from the RF load.

For S_{31_2} we have:

$$S_{31_2} = S_{31_h} \cdot S_c \cdot S_{11_{SIS1}} \cdot S_c \cdot S_{41_h} \cdot S_{11_{load}}$$

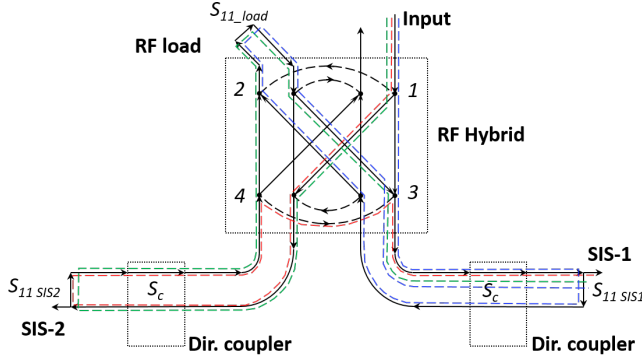


Fig. 9. Flow chart of the hybrid block showing the signal paths for $S_{31,2}$ (blue dashed path), $S_{31,3}$ (green dashed path) and $S_{31,4}$ (path colored red). Ports 1 to 4 correspond to the hybrid ports. Signs "SIS-1" and "SIS-2" indicate the location of the SIS junctions.

$$\cdot S_{41_h} \cdot S_c \cdot S_{21_SIS1} \cdot e^{i2\pi f V_p / 2L_1}, \quad (3)$$

here S_{41_h} is the S_{41} parameter of the hybrid corresponding to the cross path through ($S_{41} = S_{14} = S_{23} = S_{32}$), S_{11_load} is the reflection from the RF load, f is a frequency, V_p is the phase velocity in the waveguide and L_1 is the path length from SIS mixers to the RF load, which is close to 50 mm. For $S_{31,3}$ it will be:

$$S_{31,3} = S_{41_h} \cdot S_c \cdot S_{11_SIS2} \cdot S_c \cdot S_{31_h} \cdot S_{11_load} \cdot S_{41_h} \cdot S_c \cdot S_{21_SIS1} \cdot e^{i2\pi f V_p / 2L_1}, \quad (4)$$

here S_{11_SIS2} is the reflection from SIS mixer 2.

At last, "the second way" interference signal arriving to the SIS device 1 through the hybrid isolation after reflection from the SIS2 (red dashed path in Fig.9) can be expressed as:

$$S_{31,4} = S_{41_h} \cdot S_c \cdot S_{11_SIS2} \cdot S_c \cdot S_{21_h} \cdot S_c \cdot S_{21_SIS1} \cdot e^{i2\pi f V_p / 2L_2}, \quad (5)$$

here S_{21_h} is the hybrid S_{21} , i.e. isolation, and L_2 is the path length between the SIS mixers through the hybrid isolation, L_2 is about 33 mm.

Finally, from equations (2)-(5) we have the total S_{31} as a sum of all four parts:

$$S_{31} = S_{31,1} + S_{31,2} + S_{31,3} + S_{31,4}. \quad (6)$$

The coupling coefficient S_{41} for SIS device 2 can be derived in a similar way:

$$S_{41} = S_{41,1} + S_{41,2} + S_{41,3} + S_{41,4}. \quad (7)$$

Where:

$$S_{41,1} = S_{41_h} \cdot S_c \cdot S_{21_SIS2}, \quad (8)$$

here S_{21_SIS2} is the coupling coefficient to SIS mixer 2.

The first part of "the first way" interference signal is:

$$S_{41,2} = S_{41_h} \cdot S_c \cdot S_{11_SIS2} \cdot S_c \cdot S_{31_h} \cdot S_{11_load} \cdot S_{31_h} \cdot S_c \cdot S_{21_SIS2} \cdot e^{i2\pi f V_p / 2L_1}. \quad (9)$$

The second part will be:

$$S_{41,3} = S_{31_h} \cdot S_c \cdot S_{11_SIS1} \cdot S_c \cdot S_{41_h} \cdot S_{11_load} \cdot S_{31_h} \cdot S_c \cdot S_{21_SIS2} \cdot e^{i2\pi f V_p / 2L_1}, \quad (10)$$

And finally, "the second way" interference signal arriving to the SIS device 2 is:

$$S_{41,4} = S_{31_h} \cdot S_c \cdot S_{11_SIS1} \cdot S_c \cdot S_{21_h} \cdot S_c \cdot S_{21_SIS2} \cdot e^{i2\pi f V_p / 2L_2}. \quad (11)$$

For simplification we put $S_{11_SIS1} = S_{11_SIS2}$ and $S_{21_SIS1} = S_{21_SIS2}$ as it was done also in the simulations of the entire waveguide structure.

It is important to note that the phase velocity V_p varies with frequency:

$$V_p = \frac{c}{\sqrt{1 - (f_c/f)^2}}, \quad (12)$$

here c is the speed of light, f_c is the waveguide cutoff frequency of 150 GHz.

The described model does not include any waveguide losses, but it can be effortlessly inserted.

Based on S_{31} and S_{41} given by formulas 6 and 7 the amplitude balance, phase balance and the corresponding SRR was calculated and compared with the direct simulations. The results are presented in Fig.10.

In Fig.10 one can observe that the analytical model has a perfect qualitative and a good quantitative agreement with the direct 3D electromagnetic simulations. This proves the described concept of the waveguide structure balance. Minor discrepancies between the blue and red curves on the plots could be explained by smaller reflections, for example from the LO couplers, or by a second order reflections, which are not taken into account in the analytical model. However, their impact is not significant, and the analytical approach can be employed to develop the design, whilst the full structure simulations can be used for the final verification. Formulas similar to (2)-(11) can also be derived for LO balance to analytically reproduce the curves presented in Fig.7.

It is important to note that the coupling coefficients S_{31} and S_{41} provided by equations (6) and (7) do not present the exact structure S-parameters, as not all the symmetrical reflections are accounted here. S_{31} and S_{41} take into account only the major asymmetrical contributions. Individually, these parameters are uninteresting. However, their ratio provides correct amplitude balance, phase balance, and SRR level, resulting in valuable and objective physical parameters.

IV. RESULTS

Based on the described models, we can simulated the expected SRR performance for the presented in Fig.2 and 3 design. Let us suggest the SIS mixer reflection to be about -6.8 dB and the load reflection of -20 dB. In this scenario the SRR level will go up to -20 dB in the peaks (see Fig.11 curve 1), while the hybrid alone would provide a maximum of -26 dB. Taking into account the LO imbalance is a complex task. Fig.7 data allows us to estimate the maximum LO phase

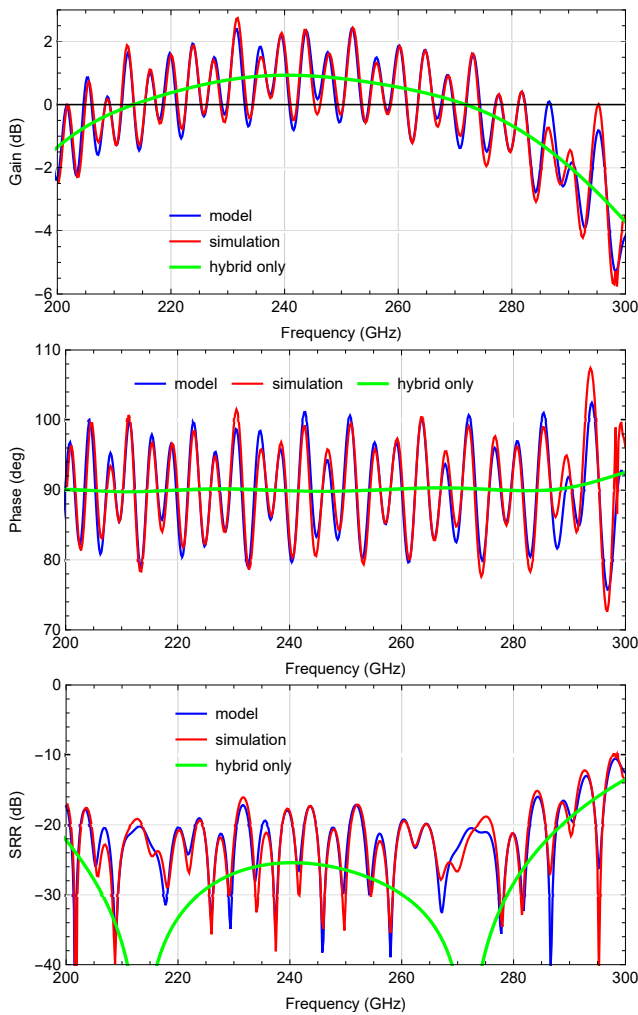


Fig. 10. Comparison of the calculated and simulated amplitude balance (top plot), phase balance (middle plot) and the SRR curve for the entire waveguide structure. Blue curves are analytically modeled and red curves are results of simulation. The green curves show the SIS reflection of -3.3 dB and -9.2 dB respectively, while RF load reflection stays about -20 dB. Green curves show as a reference the single hybrid performance.

imbalance as 5 degrees and the "bad case" LO gain error as 0.5 dB. The gain error is not so critical, because SIS mixers at the operational point are in a relative saturation and the output gain can be rather immune to the LO power variations. Moreover, the LO phase and amplitude errors shift in frequency in such a way, that only one of them can be at the peak at the same time. Keeping that in mind we can estimate the worst effect of the LO imbalance as a 5 degrees phase shift. This phase shift can be easily added analytically to either S_{31} or S_{41} . The corresponding SRR pattern is shown in Fig.11 by curve 2. As conclusion, the LO imbalance can lead to a 1-2 dB degradation of SRR in the peaks to the level of about -18 dB. On top of that, the SIS mixers can easily have a difference in gain, and the tolerance analysis predicts the waveguide structure gain deviation up to 0.3 dB. Assuming 1 dB gain difference introduced by these two factors, we can add it by reducing S_{31} or S_{41} . Both cases are depicted in Fig.11 by curve 3 and curve 4. Once the added gain error is in phase with the hybrid imbalance in the center of the band we observe

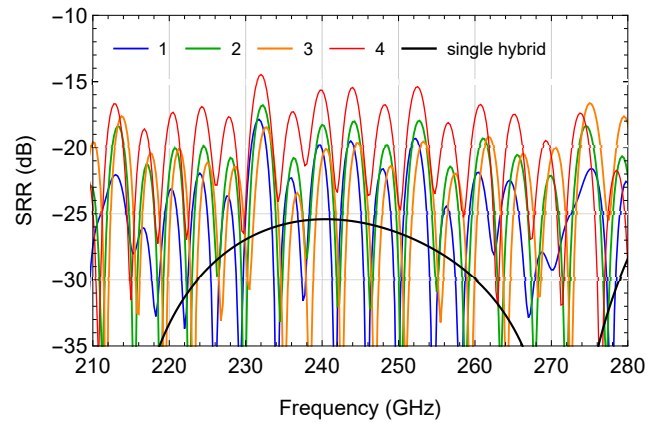


Fig. 11. Simulated SRR curves for various conditions. Curve 1 - only reflections from the SIS mixers and RF load are taken into account, curve 2 - compared to curve 1 the phase imbalance of 5 degrees is added. Curve 3 - compared to curve 2 the gain imbalance is added by increasing S_{31} by a factor of 1.1; curve 4 - 3 compared to curve 2 the imbalance is reduced by decreasing S_{31} by a factor of 1.1. The SIS reflection is -6.7 dB in all cases, while the RF load reflection is about -20 dB. Black curve shows the single hybrid performance as a reference.

SRR degradation as shown by curve 4. At the same time, the compensation of the two factors is causing the improvement of SRR level for curve 3 in the center of the band with a minor increment at the edges of the band. The described example demonstrates how complicated can be the situation even by taking into account only the given parameters.

In conclusion, for the given design the SRR level can easily rise to the level of -18 dB or even further by taking into account realistic levels of reflections and imbalances.

The model and analysis presented in this study allow for the fast and comprehensive evaluation of the SRR level for any particular mixer. This evaluation can include SIS mixer reflection, SIS mixer gain difference, hybrid amplitude balance, hybrid isolation, RF load reflection, and other relevant variables.

This paper assumes that there is negligible reflection from the input port. This is similar to the situation where a separate 2SB mixer comes equipped with a horn, like it is done for the 600-720 GHz receiver with an optical polarization split [15]. On the other hand, most of modern 2SB SIS receivers are equipped with a waveguide OMT polarization splitter. Such a splitter can easily give approximately -20 dB reflection in the input port of 2SB waveguide structure. The impact of such a reflection will be relatively small for the signal balance, because in "the first way" reflection, as described in subsection III-A, the signals reflected from SIS mixers are directed to the RF load due to interference in the Hybrid. Only the difference signal goes to the input port, making it much smaller. However, if the RF load reflection can be optimized to -30 dB, the OMT must be considered. The situation becomes even more complicated in the case of LO imbalance. If the OMT and RF load reflection are equal in magnitude and distance, they can cancel each other out due to the total symmetry of the structure. Otherwise, the interference of these two reflections will produce an even more complex periodic pattern. In any case, the OMT reflection for a particular 2SB receiver should

be accounted for and modelled. All of this will be subject to separate study.

V. CONCLUSIONS

We have modeled the entire waveguide structure of a 2SB SIS mixer and developed an analytical model predicting the SRR pattern determined by the RF part. For the first time, the mechanisms behind SRR degradation due to multiple reflections are clearly shown.

Controlling the SIS mixer reflection level is difficult since it is usually designed to provide the best sensitivity at the expense of sacrificing other parameters. Given this fact, the main focus of RF design should be on reducing hybrid isolation and minimizing RF load reflection levels. Doing so alongside maintaining the hybrid balance within a 1 dB error threshold should lead to the best SRR performance. The waveguide structure for the 2SB SIS mixer for the 211-275 GHz band was designed based on that recommendation.

The presented analysis clarifies the difficulties in achieving the -10 dB SRR specification for different ALMA receivers, despite almost perfectly balanced RF and IF hybrids.

The analytical model speeds up the optimization process by only requiring simulation of a few waveguide parts, instead of the entire structure, to estimate the SRR quality. Combining this model with a similar one for the IF part is straightforward. The full model will comprehensively describe the SRR pattern of the 2SB SIS receiver, close to the experiment, which has never been demonstrated before.

ACKNOWLEDGMENT

We would like to acknowledge Mariëlle Bekema and Rob de Haan Stijkel (Kapteyn Astronomical Institute) for their help integrating the mixer assembly. Also, we thank Sergey Likhschev and Roman Chernyi for their organizational and management support.

REFERENCES

- [1] A. Wootten and A. R. Thompson, "The atacama large millimeter/submillimeter array," *Proceedings of the IEEE*, vol. 97, no. 8, pp. 1463–1471, 2009. DOI: 10.1109/JPROC.2009.2020572.
- [2] R. Güsten, R. S. Booth, C. Cesarsky, *et al.*, "APEX: The atacama pathfinder EXperiment," in *Ground-based and Airborne Telescopes*, International Society for Optics and Photonics, vol. 6267, 2006, p. 626714. DOI: 10.1117/12.670798.
- [3] W. Wild and J. Payne, *Specifications for the alma front end assembly*, 2000.
- [4] A. R. Kerr, S.-K. Pan, S. M. Claude, P. Dindo, A. W. Lichtenberger, and E. F. Lauria, "Development of the alma-north america sideband-separating sis mixers," in *2013 IEEE MTT-S International Microwave Symposium Digest (MTT)*, IEEE, 2013, pp. 1–4.
- [5] D. Maier, J. Reverdy, L. Coutanson, D. Billon-Pierron, C. Boucher, and A. Barbier, "Fully integrated sideband-separating mixers for the noema receivers," *SSB*, vol. 4, no. 8, pp. 129–179, 2014.
- [6] J. R. Lepine, Z. Abraham, C. G. G. CASTRO, *et al.*, "The llama brazilian-argentinian radiotelescope project: Progress in brazil and brics collaboration," *Anais da Academia Brasileira de Ciências*, vol. 93, 2021.
- [7] I. D. Novikov, S. F. Likhachev, Y. A. Shchekinoy, *et al.*, "Objectives of the millimetron space observatory science program and technical capabilities of its realization," *Physics-Uspekhi*, vol. 64, no. 4, p. 386, 2021.
- [8] K. Rudakov, P. Dmitriev, A. Baryshev, A. Khudchenko, R. Hesper, and V. Koshelets, "Low-noise sis receivers for new radio-astronomy projects," *Radiophysics and Quantum Electronics*, vol. 62, pp. 547–555, 2019.
- [9] K. I. Rudakov, A. V. Khudchenko, L. V. Filippenko, *et al.*, "Thz range low-noise sis receivers for space and ground-based radio astronomy," *Applied Sciences*, vol. 11, no. 21, p. 10087, 2021.
- [10] A. Khudchenko, R. Hesper, A. M. Baryshev, J. Barkhof, and F. P. Mena, "Modular 2SB SIS receiver for 600–720 GHz: Performance and characterization methods," *IEEE Transactions on Terahertz Science and Technology*, vol. 7, no. 1, pp. 2–9, Jan. 2017, ISSN: 2156-342X. DOI: 10.1109/TTHZ.2016.2633528.
- [11] R. Hesper, G. Gerlofsma, F. P. Mena, M. C. Spaans, and A. M. Baryshev, "A sideband-separating mixer upgrade for ALMA band 9," in *Twentieth International Symposium on Space Terahertz Technology, Charlottesville*, Apr. 2009, pp. 257–260. [Online]. Available: <https://www.nrao.edu/meetings/isstt/papers/2009/2009257260.pdf>.
- [12] J. D. Garrett, C.-Y. E. Tong, L. Zeng, T.-J. Chen, and M.-J. Wang, "A 345 ghz sideband-separating receiver prototype with ultra-wide instantaneous bandwidth," *IEEE Transactions on Terahertz Science and Technology*, 2023.
- [13] R. Hesper, A. Khudchenko, A. M. Baryshev, J. Barkhof, and F. P. Mena, "A new high-performance sideband-separating mixer for 650 GHz," in *Society of Photo-Optical Instrumentation Engineers (SPIE) Conference Series*, vol. 9914, 2016, 99140G-1–99140G-11. DOI: 10.1117/12.2233065. [Online]. Available: <http://dx.doi.org/10.1117/12.2233065>.
- [14] R. Hesper, A. Khudchenko, A. M. Baryshev, J. Barkhof., and F. P. Mena, "A high-performance 650-GHz sideband-separating mixer – design and results," *IEEE Transactions on Terahertz Science and Technology*, vol. 7, no. 6, pp. 686–693, Nov. 2017, ISSN: 2156-342X. DOI: 10.1109/TTHZ.2017.2758270.
- [15] R. Hesper, A. Khudchenko, M. Lindemulder, *et al.*, "A deployable 600–720 GHz ALMA-type sideband-separating receiver cartridge," in *29th International Symposium on Space Terahertz Technology, Pasadena*, 2018. [Online]. Available: <https://www.nrao.edu/meetings/isstt/papers/2018/2018098103.pdf>.



Andrey Khudchenko received the M.S. degree in applied physics and mathematics and the Ph.D. degree in radiophysics from the Moscow Institute of Physics and Technology, Moscow, Russia, in 2007 and 2009, respectively.

From 2004 to 2008, he was an Engineer and, in 2009, a Researcher with the Kotel'nikov Institute of Radio Engineering and Electronics, Russian Academy of Sciences, Moscow. From 2010 to 2015, he has been an Instrument Scientist with The Netherlands Institute for Space Research SRON. Since 2015 to 2020, Instrument Scientist at the Kapteyn Astronomical Institute, University of Groningen. Since 2020, he joined Astro Space Center of Lebedev Physical Institute. The main activity is related to the development of new heterodyne THz instruments..



Andrey M. Baryshev received the Master's degree (summa cum laude) in physical quantum electronics from the Moscow Institute of Physics and Technology, Moscow, Russia, in 1993, and the Ph.D. degree from the Technical University of Delft, Delft, The Netherlands, in 2005.

He is currently a Senior Instrument Scientist. Since 1998, he has been with the SRON Low Energy Astrophysics Division and the Kapteyn Astronomical Institute, University of Groningen, Groningen, The Netherlands. Since 2000, he has been involved in a joint effort to develop the SIS receiver (600–720 GHz) for ALMA. In 2013, he became an Associate Professor of astronomical instrumentation for the far-infrared with the Kapteyn Astronomical Institute, University of Groningen. His main research interests include the areas of heterodyne and direct detectors for large focal plane arrays at THz frequencies, and quasi-optical system design and experimental verification.

Dr. Baryshev was the recipient of a Netherlands Organisation for Scientific Research-VENI grant for research on heterodyne focal plane array technology in 2008, and an EU commission Starting Researcher Grant for work on direct detector focal plane arrays in 2009.



Ivan Tretyakov received the M.S. degree in physics and the Ph.D. degree in radiophysics from the Moscow State Pedagogical University, Moscow, Russia, in 2006 and 2013, respectively.

From 2006 till current moment, he is a researcher with the Moscow State Pedagogical University, Moscow. From 2020 until now, he is also an Instrument Scientist with the Astro Space Center of Lebedev Physical Institute. The main activity is related to the development of HEB and SIS mixers and new THz and infrared devices..



Valery P. Koshelets received the M.S. degree in physics from Lomonosov Moscow State University, Moscow, Russia, in 1973, and the Ph.D. degree in radio physics and Doctor of Sciences (Habilitation) degree in physical electronics from the Kotel'nikov Institute of Radio Engineering and Electronics of the Russian Academy of Sciences, Moscow, in 1978 and 1990, respectively. Since 1973, he has been with the Kotel'nikov Institute of Radio Engineering and Electronics of the Russian Academy of Sciences, Moscow, Russia, where he is currently the head of

the Laboratory of superconducting devices for signal detection and processing.



Ronald Hesper received the M.Sc. degree in experimental solid state physics from the University of Leiden, Leiden, The Netherlands, and the Ph.D. degree in experimental solid state physics from the University of Groningen, Groningen, The Netherlands.

Since 2000, he has been an Instrument Scientist with the Kapteyn Astronomical Institute, University of Groningen. From 2000 to 2008, he was involved in the technological development of the ALMA Band 9 receivers, including the process of industrialization, as well as related projects like the CHAMP+ mixer arrays for APEX; from 2008 to 2013, on the development of a sideband-separating mixer upgrade for the ALMA Band 9 receivers; and from 2013 to the beginning of 2015, on the industrialization of the ALMA Band 5 receivers. Currently, he is involved in the development of new heterodyne detector technologies and industrialization of the ALMA Band 2 receivers.